JOURNAL OF SYNCHROTRON RADIATION
ISSN 1600-5775

Ultra-short and ultra-intense X-ray free-electron laser single pulse in one-dimensional photonic crystals

Jean-Michel André[a,b] and Philippe Jonnard[a,b]*

[a]Laboratoire de Chimie Physique-Matière et Rayonnement, Sorbonne Universités, UPMC Université Paris 06, Boîte courrier 1140, 4 place Jussieu, F-75252 Paris Cedex 05, France, and [b]Laboratoire de Chimie Physique-Matière et Rayonnement, CNRS UMR 7614, Boîte courrier 1140, 4 place Jussieu, F-75252 Paris Cedex 05, France. *Correspondence e-mail: philippe.jonnard@upmc.fr

Received 1 September 2016
Accepted 17 January 2017

Edited by G. Grübel, HASYLAB at DESY, Germany

Keywords: X-ray free electron laser; one-dimensional photonic crystal; non-linear processes.

The propagation within a one-dimensional photonic crystal of a single ultra-short and ultra-intense pulse delivered by an X-ray free-electron laser is analysed with the framework of the time-dependent coupled-wave theory in non-linear media. It is shown that the reflection and the transmission of an ultra-short pulse present a transient period conditioned by the extinction length and also the thickness of the structure for transmission. For ultra-intense pulses, non-linear effects are expected: they could give rise to numerous phenomena, bi-stability, self-induced transparency, gap solitons, switching, *etc.*, which have been previously shown in the optical domain.

1. Introduction

The purpose of this work is to analyse different aspects of the time-domain propagation of an ultra-intense and/or ultra-short single pulse delivered by an X-ray free-electron laser (X-FEL) within a Bragg structure. In the hard X-ray domain, the Bragg structures firstly implemented were natural crystals, and the steady-state (time-independent) diffraction by crystals was studied in detail within the framework of the so-called dynamical theory of diffraction (Authier, 2003). Since the 1970s, synthetic Bragg crystals based on periodic multilayer stacks, sometimes called multilayer interferential mirrors (MIMs), have been developed for the soft X-ray domain for which natural crystals were unusable; the time-independent diffraction by these multilayer structures have also been extensively studied (Pardo *et al.*, 1988).

In this paper, we consider a MIM but some conclusions could be drawn in a similar way to the case of a natural crystal diffracting in the Bragg (reflection) or Laue (transmission) geometry where only one dimension is involved. Thus, hereafter, we use the generic term 'one-dimensional photonic crystal' (1D-PC) to refer to the two types of Bragg structures, crystal or MIM. The term 'distributed-feedback structure' (DFB) has also been commonly used in the literature to refer to this kind of structure. Let us outline that the terminologies PC and DFB are rarely used for the X-ray range but are more common in the long-wavelength domain (optical range, *etc.*). Indeed most of the effects that we describe in this paper for the X-ray domain can be found throughout the whole electromagnetic spectrum and in particular the non-linear (NL) processes have been studied in detail in the optical domain mainly in the context of optics of fibers and waveguide Bragg gratings, so that a large part of §4 is borrowed from the

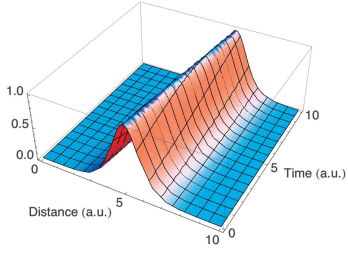

numerous studies published on these topics. The objective of the present work is mainly to inform the community of X-FEL users about some linear and NL effects that could be shown with X-FEL radiation pulses.

The X-FEL facilities are now able to deliver single ultra-intense and ultra-short pulses of coherent radiation; considering for instance the FERMI facility, the photon beam parameters for FEL1 are 100 μJ per pulse with an estimated pulse length (FWHM) of less than 150 fs. 'Ultra-short' means that the duration of the pulse is less that the relaxation times of the media, 'ultra-intense' means that non-linear optical effects are expected, and finally 'coherence' means that the photons in a pulse have fixed phase relationships forming a single mode. All these unique features (high brightness, short time duration, temporal and spatial coherence) open the way to the observation of coherent NL processes. The induced polarization **P** of the materials is given as a power-series expansion of the incident electric field **E**, in cgs units,

$$\mathbf{P} = 4\pi \sum_{i \geq 1} \chi^{(i)} |\mathbf{E}|^{i-1} \mathbf{E}, \tag{1}$$

$\chi^{(i)}$ being the susceptibility of the ith order. Generally, the even-order terms are null for any centro-symmetric system so that the lowest-order NL processes are of the third order. Among them, the most famous one is the Kerr effect for which the refractive index change is proportional to the square of the applied electric field or electric field intensity. Recently, X-ray reflectivity enhancement in titanium has been reported (Bencivenga *et al.*, 2014) by a team using ultrafast XUV radiation at the TIMEX end-station of the EIS beamline of the FERMI X-FEL facility; the experimental results have been interpreted as a dependence of the plasma frequency with respect to the energy density $\bar{E} \simeq |\mathbf{E}|^2$ which leads in the framework of the Drude refractive index model to variation of reflection upon the deposited energy density. The dependence of the refractive index upon $\bar{E}$ can be regarded as a special case of the Kerr effect known as refractive index intensity dependence which can give rise to numerous NL effects observed and expected especially in the low-energy domain of the electromagnetic spectrum: self-focusing, self-phase modulation, spatial solitons (New, 2014), NL surface polaritons (Leung, 1985). The intensity-dependent refractive index is also at the origin, in the Bragg structure, of various effects such as gap solitons (Chen & Mills, 1987; Mills & Trullinger, 1987; Martijn de Sterke & Sipe, 1994) connected to self-induced transparency (Aceves & Wabnitz, 1989), pulse compression in Bragg optical fiber (Winful, 1985), and bistability in NL distributed feedback structure (Winful *et al.*, 1979).

Time-dependent diffraction by a Bragg structure has received comparatively poor attention: Chukhovskii & Förster have considered time-dependent diffraction by a crystal (Chukhovskii & Förster, 1995) and more recently their approach has been extended to a 1D-PC (André & Jonnard, 2015). Let us mention that the response of Bragg structures, MIMs (Ksenzov *et al.*, 2008, 2009; Bushuev & Samoylova, 2011) and crystals (Shastri *et al.*, 2001; Bushuev, 2008), to X-FEL sources has been treated by means of methods implemented for the frequency domain.

We lead our investigation in the framework of the time-dependent coupled-wave (TDCW) analysis extended to NL materials. In §2 we establish the system of coupled-wave equations taking into account the NL response of the media. In §3 we consider the low-intensity regime, where NL behaviour can be neglected; we show that the indicial response of a MIM displays a transient period determined by the extinction length of the Bragg structure in terms of reflection and by the extinction length combined with the thickness of the structure in terms of transmission. In §4 we consider the high-intensity regime, with NL effects first in the steady-state case where bistability can be envisaged, then in the time-dependent case where we consider the possibility to observe Bragg solitons associated with a kind of self-induced transparency of the Bragg structure.

2. Time-dependent coupled-wave theory in non-linear 1D-PC

We consider the propagation of an ultra-short and ultra-intense (generally coherent) single pulse such as the one delivered by an X-FEL in a 1D-PC shown in Fig. 1. The figure also gives the geometry of the problem and some notations. We consider a periodic stack of N bilayers. The bilayer is made up of a material a with dielectric susceptibility χ_a and material b with dielectric susceptibility χ_b with layer thickness $d_a = \gamma d$ and $d_b = (1 - \gamma)d$, respectively. The incoming radiation with a wavevector $\mathbf{k} = (k_x, k_z)$ in the plane (x, z) strikes the multilayer structure under a glancing angle θ. A Cartesian orthogonal reference frame $(\hat{\mathbf{x}}, \hat{\mathbf{y}}, \hat{\mathbf{z}})$ is used. L is the total thickness of the stack, equal to Nd. The reciprocal vector $\mathbf{g} = (2\pi/d)\hat{\mathbf{z}}$ is orthogonal to the stratification planes.

The electric field $\mathbf{E}(x, z, t)$ of the X-FEL single pulse is modelled by a quickly varying carrier with frequency $\omega = \chi\kappa$, modulated by an envelope $E_0(z, t)$, and we write it as follows (assuming a s-polarization case),

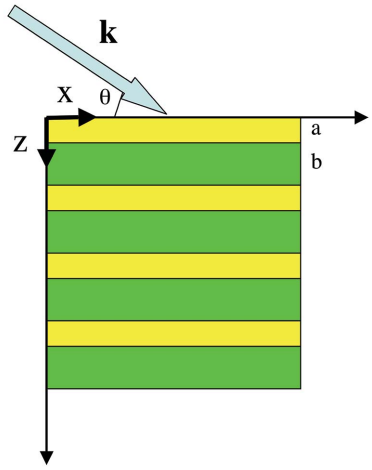

Figure 1
Sketch of the 1D-PC consisting of a periodic stack of alternating a/b bilayers.

$$\mathbf{E}(x, z, t) = E_0(z, t)\exp\left[i(k_x x - \omega t)\right]\hat{\mathbf{y}}. \tag{2}$$

We assume that the polarization of the media follows instantly the change of the electric field but that the media have a NL behaviour; more precisely, we consider that the medium is subject to the special case of the optical Kerr effect for which the refractive index is intensity-dependent. Consequently, we write the polarization $\mathbf{P}$ as follows,

$$\begin{aligned}\mathbf{P}(x, z, t) &= \chi\left[z, E_0(z, t)\right]\mathbf{E}(z, t)\\ &= \left[\chi^{(1)}(z) + \chi^{(3)}(z)\left|E_0(z, t)\right|^2\right]\\ &\quad\times E_0(z, t)\exp\left[i(k_x x - \omega t)\right]\hat{\mathbf{y}},\end{aligned} \tag{3}$$

that corresponds to a third-order NL. The susceptibilities $\chi^{(n)}(z)$ do not depend on time while the total susceptibility χ depends on time through $E_0(z, t)$, but they vary periodically along the z direction. Consequently they can be expanded in a Fourier series,

$$\chi^{(n)}(z) = \bar{\chi}^{(n)} + \sum_{p=-\infty}^{+\infty}\Delta\chi^{(n)}u_p\exp(ipgz), \tag{4a}$$

with

$$\bar{\chi}^{(n)} = \chi_a^{(n)}\gamma + \chi_b^{(n)}(1-\gamma), \tag{4b}$$

$$\Delta\chi^{(n)} = \chi_a^{(n)} - \chi_b^{(n)} \ll \bar{\chi}^{(n)}, \tag{4c}$$

$$u_p = \gamma\,\mathrm{sinc}(\pi p\gamma)\exp(-i\pi p\gamma), \tag{4d}$$

$$g = 2\pi/d. \tag{4e}$$

In our study we restrict to the Kerr NL and consequently we keep only the terms $\bar{\chi}^{(1)}$, $\bar{\chi}^{(3)}$, $\Delta\chi^{(1)}$ and $\Delta\chi^{(3)}$.

In the 1D-PC, the electric field envelope can be written as the superposition of two contra-propagating waves along the z-axis,

$$E_0(z, t) = F(z, t)\exp(+i\kappa z) + B(z, t)\exp(-i\kappa z), \tag{5a}$$

with

$$\kappa = k\sin\theta, \tag{5b}$$

and using the following auxiliary amplitude terms

$$\mathcal{E}_+(z, t) = F(z, t)\exp\left[-i\left(\frac{pg}{2} - \kappa\right)z\right] \tag{6a}$$

and

$$\mathcal{E}_-(z, t) = B(z, t)\exp\left[+i\left(\frac{pg}{2} - \kappa\right)z\right]. \tag{6b}$$

In the framework of the two-wave theory where only the zeroth-order and the pth Fourier term are strongly coupled (*i.e.* in the vicinity of the pth Bragg resonance), it can be shown that, in the slow-varying approximation both in space and in time, the column amplitude vector

$$\bar{\mathcal{E}}(z, t) = \begin{bmatrix}\mathcal{E}_+(z, t)\\ \mathcal{E}_-(z, t)\end{bmatrix}$$

and its complex conjugate

$$\bar{\mathcal{E}}^*(z, t) = \begin{bmatrix}\mathcal{E}_+^*(z, t)\\ \mathcal{E}_-^*(z, t)\end{bmatrix}$$

obey the following system of partial differential equations (PDEs) forming the so-called non-linear coupled mode equations with loss or gain,

$$\begin{aligned}\partial_z\bar{\mathcal{E}}(z, t) &= \bar{\mathcal{T}}\partial_t\bar{\mathcal{E}}(z, t) + i\bar{\mathcal{M}}\,\bar{\mathcal{E}}(z, t)\\ &\quad + \bar{\mathcal{N}}\,\bar{\mathcal{E}}(z, t) + \bar{\mathcal{N}}_c\,\bar{\mathcal{E}}^*(z, t),\end{aligned} \tag{7}$$

where $\bar{\mathcal{M}}$ is the propagation matrix in space given by

$$\bar{\mathcal{M}} = \begin{pmatrix}-\alpha & K^+\\ K^- & \alpha\end{pmatrix}, \tag{8a}$$

with

$$\alpha = \frac{pg}{2} + \frac{k^2}{\kappa}\,2\pi\bar{\chi}^{(1)} - \kappa, \tag{8b}$$

$$K^+ = -\frac{k^2}{\kappa}2\pi\Delta\chi^{(1)}u_p, \tag{8c}$$

$$K^- = \frac{k^2}{\kappa}2\pi\Delta\chi^{(1)}u_{-p}. \tag{8d}$$

$\bar{\mathcal{T}}$ is the propagation matrix in time,

$$\bar{\mathcal{T}} = \begin{pmatrix}-\frac{1}{c\sin\theta} & 0\\ 0 & \frac{1}{c\sin\theta}\end{pmatrix}. \tag{9a}$$

$\bar{\mathcal{N}}$ is the NL matrix corresponding to the average NL term,

$$\bar{\mathcal{N}} = \begin{bmatrix}-\Gamma_a\Lambda_+(z, t, S, X) & \Gamma_{p\Delta}\Lambda_-(z, t, S, X)\\ -\Gamma_{p\Delta}\Lambda_+(z, t, S, X) & \Gamma_a\Lambda_-(z, t, S, X)\end{bmatrix}, \tag{9b}$$

with

$$\Lambda_+(z, t, S, X) = S\left|\mathcal{E}_+(z, t)\right|^2 + 2X\left|\mathcal{E}_-(z, t)\right|^2, \tag{9c}$$

$$\Lambda_-(z, t, S, X) = S\left|\mathcal{E}_-(z, t)\right|^2 + 2X\left|\mathcal{E}_+(z, t)\right|^2. \tag{9d}$$

The quantity S corresponds to the self-phase (SP) modulation term while the quantity X is for the cross-phase (CP) modulation; moreover, the term Γ_a corresponds to the average NL term while the term $\Gamma_{p\Delta}$ is associated with the pth Fourier component of the NL term of the dielectric susceptibility $\Delta\chi^{(3)}u_p$.

The matrix $\bar{\mathcal{N}}_c$ affecting $\bar{\mathcal{E}}^*(z, t)$ is

$$\bar{\mathcal{N}}_c = \Gamma_m\begin{bmatrix}\mathcal{E}_-(z, t)^2 & 0\\ 0 & -\mathcal{E}_+(z, t)^2\end{bmatrix}. \tag{10}$$

The coefficient Γ_m is also related to the third-order dielectric susceptibility. It contributes to the wave-mixing process. If the polarization is stationary according to our assumption, one can show that in our geometry

$$S = X = 1, \qquad \Gamma_a = \Gamma_m \propto 1 + 4\pi\bar{\chi}^{(3)}. \tag{11}$$

The loss (or gain) has been taken into account in the above theory by introducing an imaginary part in the dielectric constants. Generally, in the X-ray domain, materials are absorbing; nevertheless, stimulated emission has been

reported in solids (silicon and magnesium oxide) under X-FEL excitation (Beye *et al.*, 2013; Yoneda *et al.*, 2015; Jonnard *et al.*, 2016), so that the case of a medium with gain (lasing medium) needs to be considered too. Let us mention that X-UV lasing in a 1D-PC with pumping by X-FEL, forming a so-called distributed feedback laser, has been recently examined (André *et al.*, 2014).

3. Low-intensity regime: transient response

In this section we assume that the intensity of the X-FEL radiation is low enough so that no NL behaviour occurs: this is the low-intensity regime (LIR). We will see that, even if the response of the 1D-PC to the pulse is then purely linear, notable effects occur when the time width of the pulse is very short. First we will consider the so-called impulse and indicial response of the 1D-PC in terms of reflection and transmission; the impulse response corresponds to an incident Dirac-δ pulse while the indicial response corresponds to an incident step-like Heaviside-Θ signal in terms of time dependence. The 1D-PC is assumed to work at the Bragg resonance.

Under the LIR, the system of PDEs, equation (7), is linear and can be reduced by means of the following characteristic coordinates v, w,

$$v = \frac{1}{2}(ct\sin\theta - z), \tag{12a}$$

$$w = \frac{1}{2}(ct\sin\theta + z), \tag{12b}$$

and the reduced field amplitudes defined by

$$\mathcal{E}_+(z,t) = \exp(-i\alpha ct\sin\theta)\,\tilde{f}(v,w), \tag{13a}$$

$$\mathcal{E}_-(z,t) = \exp(-i\alpha ct\sin\theta)\,\tilde{b}(v,w), \tag{13b}$$

to the following hyperbolic second-order PDE,

$$\mathcal{L}_{(v,w)}\big[\tilde{f}(v,w);\tilde{b}(v,w)\big] = 0 \tag{14}$$

where $\mathcal{L}_{(v,w)}$ is the differential operator defined by

$$\mathcal{L}_{(v,w)} = \left(\frac{\partial^2}{\partial v\partial w} + \frac{\pi^2}{\Lambda^2}\right), \tag{15}$$

with Λ^2 the quantity related to the coupling constants K^+, K^- by

$$\Lambda^2 = -\frac{\pi^2}{K^+K^-}. \tag{16}$$

The quantity Λ is the extinction length of the dynamical theory of diffraction. For given boundary conditions, the PDE given by equation (14) can be solved by implementing Riemann's method (Courant & Hilbert, 1965). This method requires an integration contour in the characteristic coordinate plane shown in Fig. 2.

Application of Riemann's method leads to writing the backward propagating (reflected) field as follows,

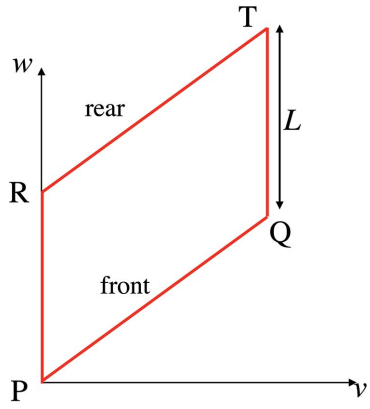

Figure 2
1D-PC geometry in the characteristic coordinate reference frame (v, w); the front surface is given by $w = v$ (line PQ) while the rear surface is given by $w = v + L$ (line RT).

$$\tilde{b}(v,v) = -iK^-\frac{\Lambda}{\pi}\int_P^Q \frac{J_1[(2\pi/\Lambda)(v-v')]}{(v-v')}\,\tilde{f}(v',v')\,\mathrm{d}v', \tag{17}$$

where $\tilde{f}(v',v')$ corresponds to the incoming (forward propagating) wave at the front surface ($z = 0$). J_1 is the Bessel function of the first kind. From equation (17) one can deduce the impulse in terms of reflection coefficient. The impulse incident reduced field amplitude $\tilde{f}(v,v)_\delta$ can be written as

$$\tilde{f}(v,v)_\delta = \frac{\exp(+i2\alpha v)}{\sqrt{2\pi}}\,\frac{\sin\theta}{2}\,\delta\left[\frac{x\cos\theta\sin\theta}{2} - v\right], \tag{18}$$

where δ stands for the Dirac peak. Inserting equation (18) into (17) and performing the integration gives, for the reduced diffracted field $\tilde{b}(v,v)_\delta$ under the incidence of a Dirac pulse,

$$\tilde{b}(v,v)_\delta = -i\sin\theta\,K^-\frac{\Lambda}{\pi}\,\frac{\exp(+iax\cos\theta\sin\theta)}{\sqrt{2\pi}} \times \frac{J_1[(\pi/\Lambda)\sin\theta(ct - x\cos\theta)]}{\sin\theta(ct - x\cos\theta)}, \tag{19}$$

that is, for the diffracted field,

$$\mathcal{E}_-(z=0,T)_\delta = i\sin\theta\,K^-\frac{\Lambda}{\pi\sqrt{2\pi}}\,\frac{J_1[\zeta(T)]}{\zeta(T)}\,\Theta(T),$$
$$\zeta(T) = (\pi/\Lambda)\sin\theta\,cT, \tag{20}$$

where the time delay T has been introduced, measured with respect to the diffracted wave plane,

$$T = \frac{ct - x\cos\theta}{c}. \tag{21}$$

$\hat{R}_\delta(T) = \mathcal{E}_-(z=0,T)_\delta$ is the impulse response in terms of reflection and also the temporal Green function $g_R(T)$ for reflection. For time coherent radiation with time-dependent causal distribution Ξ (normalized to unity), the indicial response $\hat{R}_\Theta(t)$ in terms of reflection coefficient is given by

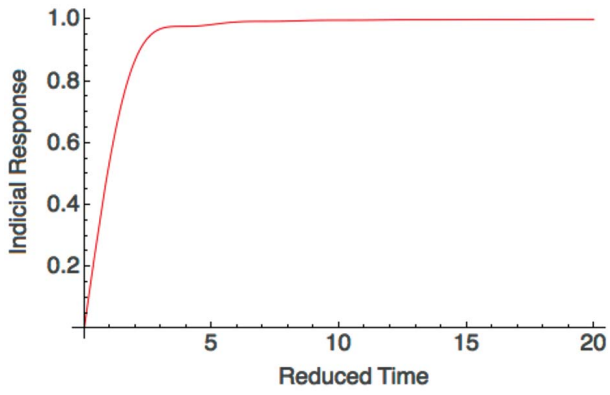

Figure 3
Indicial response in terms of peak reflectance *versus* reduced time for a 1D-PC at the Bragg resonance (Bragg angle). The response is normalized to unity.

$$\hat{R}_\Theta(t) = \int_{-\infty}^{+\infty} |g_R(T)|^2\, \Xi(t-T)\, \mathrm{d}T = \int_0^t |g_R(T)|^2\, \Xi(t-T)\, \mathrm{d}T. \tag{22}$$

Equation (22) allows one to draw a 'universal' curve in terms of peak reflectance for the indicial response $\hat{R}_\Theta(t)$ *versus* the reduced time $\bar{t} = t(\pi \sin\theta\, c/\Lambda)$ (see Fig. 3). It appears that the indicial response for reflection is conditioned by the extinction length Λ and that it presents a transient period whose duration is given by a characteristic transient time t_c approximately equal to two units of reduced time.

Following a similar calculation it is possible to show that the forward propagating transmitted field $\tilde{f}(v, w)]_T$ is given by

$$\tilde{f}(v, w)]_T \simeq -\frac{2\pi^2 L}{\Lambda^2} \int_P^Q \tilde{f}(v', v') \times \frac{J_1\{(2\pi/\Lambda)[(v + L - v')(v - v')]^{1/2}\}}{(2\pi/\Lambda)[(v + L - v')(v - v')]^{1/2}}\, \mathrm{d}v'. \tag{23}$$

To determine the impulse response in terms of transmission, we insert into equation (22) the expression of the incident pulse given by equation (18) as for the reflection case and we perform the integration as for the reflection geometry, resulting in the impulse response in terms of transmission $\hat{T}_\delta(t)$ being $\mathcal{E}_+(z = L, T)_\delta$,

$$\mathcal{E}_+(z = L, T)_\delta = \frac{\pi^2 L}{\sin\theta \Lambda^2} \frac{J_1[\xi(T)]}{\xi(T)}\, \Theta(T), \qquad \xi(T) = \frac{\pi}{\Lambda}\left[cT\left(\frac{2L}{\sin\theta} + \frac{cT}{\sin\theta^2}\right)\right]^{1/2}. \tag{24}$$

For time-coherent radiation with time-dependent causal distribution Ξ the indicial response $\hat{T}_\Theta(t)$ in terms of transmission coefficient is given from the temporal Green function for transmission, $g_T = \hat{T}_\delta$,

$$\hat{T}_\Theta(t) = \int_{-\infty}^{+\infty} |g_T(T)|^2\, \Xi(t-T)\, \mathrm{d}T = \int_0^t |g_T(T)|^2\, \Xi(t-T)\, \mathrm{d}T. \tag{25}$$

The indicial response in terms of transmission is conditioned both by the extinction length Λ and by the thickness L of the 1D-PC.

From the indicial responses of the 1D-PC it is possible to calculate the time-dependent reflection and transmission of a short pulse. Let $I(t)$ be the temporal envelope shape of any incident pulse and $O(t)$ the envelope of the corresponding reflected or transmitted pulse. Then the Laplace transform $O(s)$ of $O(t)$ is related to the Laplace transform $I(s)$ of $I(t)$ by means of the convolution theorem,

$$O(s) = \hat{Z}_\delta(s)\, I(s), \tag{26}$$

$\hat{Z}_\delta(s)$ being the transfer function that is the Laplace transform of the impulse response $\hat{Z}_\delta(t)$ [$\equiv \hat{R}_\delta(t)$ or $\hat{T}_\delta(t)$]. $\hat{Z}_\delta(t)$ can be determined from $\hat{Z}_\Theta(t)$ by Strejc's method (de Larminat, 2007). By performing an inverse Laplace transform of equation (26), one determines the temporal response (André & Jonnard, 2015).

We now illustrate the previous theory in the case of a MIM consisting of a stack of $N = 7$ Ti/Si bilayers; the period d is equal to 70 nm and the γ ratio is equal to 0.5. The photon energy of the incident XFEL radiation is 20 eV ($\lambda = 62$ nm) diffracted at $\theta = 60°$. The choice of the Ti/Si system is not governed by the objective of optimizing the reflectance of the MIM but by the fact that it has been shown (see Bencivenga *et al.*, 2014) that titanium has a NL behaviour at the photon energy of interest. The temporal profile XFEL pulse is modelled by a sine-squared function; that is, the envelope of the incident pulse varies as $\sin^2[\pi(t/\tau)]$ in the time interval $[0, \tau]$ and 0 outside.

The NL dielectric constant (square of the refractive index) of titanium is assumed to be given by Drude's formula modified to account for the intensity dependence (Bencivenga *et al.*, 2014),

$$\varepsilon_{\mathrm{NL\,Ti}} = 1 - \frac{\omega_{p0}^2(1 + A\bar{E})}{\omega^2 + i\omega\bar{\gamma}} \approx \varepsilon_{\mathrm{L\,Ti}} + \Delta\varepsilon_{\mathrm{Ti}}\bar{E}, \tag{27a}$$

$$\varepsilon_{\mathrm{L\,Ti}} = 1 - \frac{\omega_{p0}^2}{\omega^2 + i\omega\bar{\gamma}} \approx 1 - \frac{\omega_{p0}^2}{\omega^2} + i\bar{\gamma}\frac{\omega_{p0}^2}{\omega^3}, \qquad \Delta\varepsilon_{\mathrm{Ti}} = -A\frac{\omega_{p0}^2}{\omega^2}, \tag{27b}$$

ω_{p0} is the plasma frequency at zero energy density ($\bar{E} = 0$) equal to 17.7 eV, A being an empirical constant equal to 7.5×10^{12} m^3 J^{-1}. Following Bencivenga *et al.* (2014), the damping term $\bar{\gamma}$ is taken to be $0.1\omega_{p0}$ as for aluminium (Ujihara, 1972) since a reference value is not available in the literature for Ti. Numerically, at 20 eV, one has

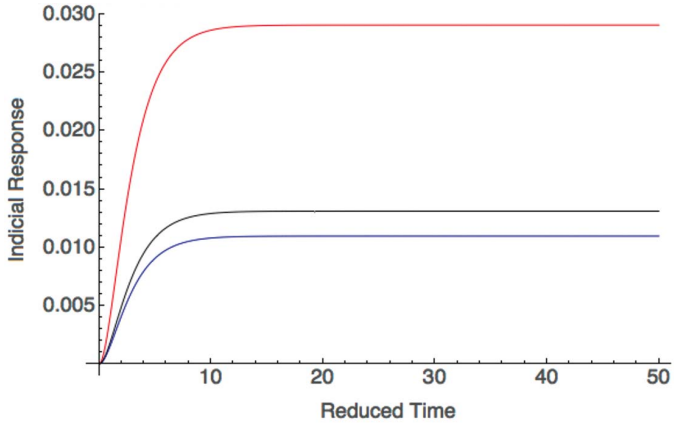

Figure 4
Indicial response of the Ti/Si MIM *versus* time in terms of peak reflectance for different glancing angles θ: red line, $\theta = 60^\circ$ (Bragg angle); black line, $\theta = 65^\circ$; blue line, $\theta = 55^\circ$.

$$\varepsilon_{\mathrm{L\,Ti}} = 0.217 + i\,0.069 = (0.474 + i\,0.087)^2,$$
$$\Delta\varepsilon_{\mathrm{Ti}} = -5.87 \times 10^{12}.$$

For silicon, from Palik (1985), at 20 eV,

$$\varepsilon_{\mathrm{L\,Si}} = (0.567 + i\,0.083)^2.$$

Fig. 4 displays the indicial response in terms of reflectance for the Ti/Si MIM under consideration, for different glancing angles close to the Bragg angle ($\theta = 60^\circ$) obtained by solving equation (7) (André & Jonnard, 2015). It appears that the transient time is around 6.5 fs to reach 90% of the stationary indicial response. The temporal response in terms of peak reflectance (that is, for resonance at Bragg angle $\theta = 60^\circ$) to a single pulse for several time widths τ (10, 50, 100 fs) is shown in Fig. 5. It can be seen that for the shortest incident pulses the reflectance does not have enough time to reach its steady-state value. For the longest pulses, the response duration is quite symmetrical and lasts about the time of the pulse. For the shortest pulse, the response is asymmetrical and lasts at least twice the time of the pulse.

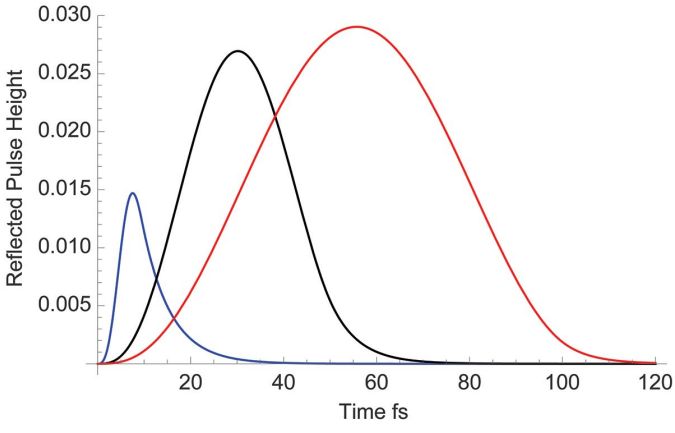

Figure 5
Reflected pulse by the Ti/Si MIM at Bragg resonance *versus* time for several time widths τ of the incident pulse: blue line, $\tau = 10$ fs; black line, $\tau = 50$ fs; red line, $\tau = 100$ fs.

4. High-intensity regime: solitons and other non-linear effects

In this section, we highlight some NL effects occurring in the high-intensity regime (HIR) where Kerr non-linearity takes place. If one starts from the general coupled wave (CW) equation, equation (7), to deal with this regime, one has to face a lot of mathematical problems that are very difficult to handle, leaving one with only numerical techniques that are generally computationally intensive and do not provide the necessary insight into the physics. So we choose to simplify the problem by keeping in equation (7) only the terms that describe the basic phenomena. In this way we restrict our study to the following cases:

(i) Loss and/or gain in the medium are discarded.

(ii) The 1D-PC is tuned at the pth Bragg resonance.

(iii) Wave mixing that is the effect of the matrix $\bar{\mathcal{N}}_c$ in equation (7) is neglected.

4.1. NL stationary case

From the study of the time-dependent linear case examined in §3, one can expect, for pulses with very large time width with respect to the characteristic time associated with the extinction length, that the propagation of the pulse in NL media can be satisfactorily described by the time-independent (stationary) form of the NL PDEs. It can be shown that under these conditions the system of hyperbolic PDEs deduced from equation (7) with the above-mentioned assumptions has two conserved quantities depending on $\mathcal{E}_+(z)$ and $\mathcal{E}_-(z)$,

(i) The intensity flow, $|\mathcal{E}_+(z)|^2 - |\mathcal{E}_-(z)|^2 = I_{\mathrm{in}} - I_{\mathrm{ref}} = I_{\mathrm{out}} \equiv T$ (see Appendix *A*);

(ii) The real-valued Hamiltonian (non-explicited).

Also, since the degree of freedom (equal to 2) of the PDE system is equal to the number of conserved quantities, by virtue of the Liouville–Arnould theorem, this PDE system is exactly integrable. With the 'standard' boundary conditions,

$$\begin{aligned} |\mathcal{E}_+(0)|^2 &= I_{\mathrm{in}}, \qquad |\mathcal{E}_-(0)|^2 = I_{\mathrm{ref}}, \\ |\mathcal{E}_+(L)|^2 &= I_{\mathrm{out}}, \qquad |\mathcal{E}_-(L)|^2 = 0, \end{aligned} \tag{28}$$

the integration yields relationships between the transmittance (reflectance) and the input intensity I_{in} in terms of Jacobi elliptic functions (see Appendix *A*). From the expression of the transmittance deduced from equation (45), it appears that the 1D-PC can present a bi-stability. This is illustrated by Fig. 6, obtained from equation (50). It shows a typical S-shape response at Bragg resonance in terms of normalized transmittance *versus* I_{in} for the value of $\bar{\kappa}L$ equal to 2; the negative slope region (between 4.75 and 4.85) is unstable. The Bragg reflectivity associated with the linear component of the dielectric constant is erased until a transparent state (reflectivity close to zero) is reached at a point T as shown in Fig. 6. For low values of $\bar{\kappa}L$, bi-stability cannot be achieved by lack of feedback but for larger values of $\bar{\kappa}L$ multiple-switching

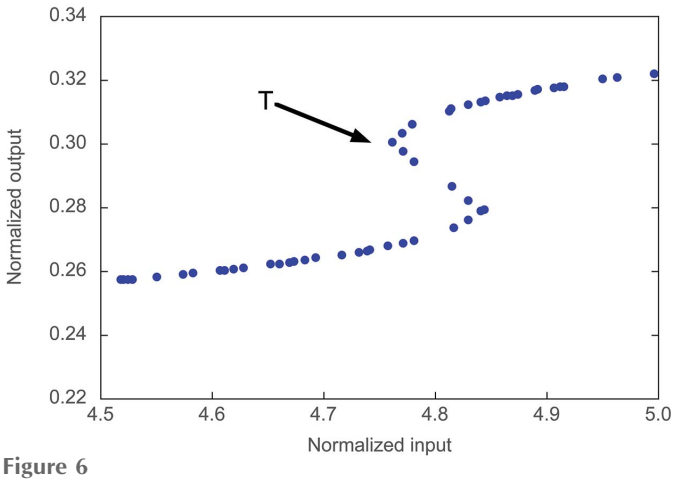

Figure 6
Transmittance *versus* normalized input intensity exhibiting bi-stability of the NL 1D-PC; a quasi-transparent state appears at the point T.

phenomena appear (Winful *et al.*, 1979). NL 1D-PC can give rise, according to the conditions, to multi-stabilities as well as optical limiting (see §4.2.2) and may even undergo chaotic behaviour.

4.2. NL time-dependent case

4.2.1. Solitons. The physics of the 1D-PC in the linear case is governed by the occurrence of two branches of the dispersion curve in the frequency domain, experiencing anti-crossing owing to the wave coupling. In the contra-propagating case relevant to our problem, the anti-crossing gives rise to a forbidden energy gap. In the LIR considered in the previous section, the Bragg frequency ω_c lies within the band gap where running waves are forbidden. At HIR, the dielectric constant changes proportionally to the electric field intensity and the branches shift down/up in energy (a kind of blue/red shift of the band gap according to positive/negative NL) so that the frequency ω_c no longer falls within the forbidden gap but shifts towards a region with allowed travelling waves. This mechanism is sketched in Fig. 7. The gap soliton and the optical limiting and switching examined hereafter are related to this mechanism.

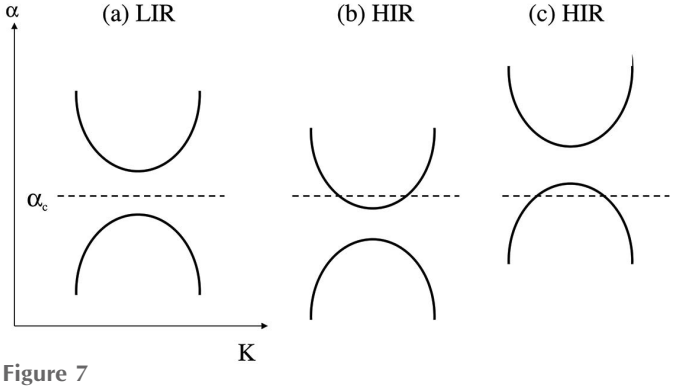

Figure 7
Dispersion curves in the frequency (ω)/Bloch wavenumber (K) domain. (*a*) LIR, (*b*) HIR and positive NL with a shift-down in frequency, (*c*) HIR and negative NL with a shift-up in frequency.

The dynamics of the system are then governed by the system of NL PDEs, equation (7). A remarkable property of this system is that the entire family of localized solutions can be built analytically forming the 'soliton-like' solutions. The adequacy of the term 'soliton' is discussed in many specialized works (see, for instance, Wazwaz, 2009); here we merely use the term soliton to mean localized solutions not in the strict mathematical sense of integrability. We first consider the case where SP is neglected ($S = 0$). Although one could imagine cases for which $X = 0$, it seems that there are no realistic geometries in which $S = 0$ and $X = 0$ so that the model under these conditions is not relevant directly in our problem. Nevertheless, the latter case paves the way to a general solution as we will see hereafter. It has been recognized that the system given by equation (6) with $S = 0$ and $X \neq 0$ reduces to the massive Thirring model (MTM) which is integrable and exhibits soliton-like solutions (Martun de Sterke & Sipe, 1994). The more general solution when the SP term is not neglected (generally $X = S$) can be built from the soliton-like solutions of the MTM (Orfanidis & Wang, 1975).

We briefly present the mathematical way to the more general [in the sense $S \neq 0$, $X \neq 0$ and $\mathrm{Im}(\varepsilon) \neq 0$ but wave mixing terms remain null] soliton-like solution of equation (6). First the column vector $\bar{\mathcal{E}}(z, t)$ without SP can be regarded as a Dirac spinor ψ and equation (6) is formally the same as the MTM equation,

$$i\gamma^{\mu}\partial_{\mu}\psi = m\psi - gJ_{\mu}\psi, \qquad J^{\mu} = \bar{\psi}\gamma^{\mu}\psi, \tag{29}$$

γ^{μ} being the gamma matrices formed from the Pauli matrices σ_{μ}. The MTM equation can be reduced to the Sine–Gordon one which is integrable; finally, the soliton-like solutions of the MTM are (Aceves & Wabnitz, 1989)

$$\psi = \begin{pmatrix} \psi_1 \\ \psi_2 \end{pmatrix}, \tag{30a}$$

with

$$\psi_1 = \pm\left(\pm\frac{\bar{\kappa}}{2\Gamma_a}\right)^{1/2}\frac{1}{\Delta}\sin Q\exp[\pm i\bar{\kappa}\zeta\cos Q] \times \mathrm{sech}[\bar{\kappa}\xi\sin Q \mp iQ/2], \tag{30b}$$

$$\psi_2 = -\left(\pm\frac{\bar{\kappa}}{2\Gamma_a}\right)^{1/2}\Delta\sin Q\exp[\pm i\bar{\kappa}\zeta\cos Q] \times \mathrm{sech}[\bar{\kappa}\xi\sin Q \pm iQ/2], \tag{30c}$$

$$\zeta = \frac{vz - t}{(1 - v^2)^{1/2}}, \tag{30d}$$

$$\xi = \frac{z - vt}{(1 - v^2)^{1/2}}. \tag{30e}$$

The signs are determined by the relative sign of the linear and NL coupling coefficients. Equations (30) represent a two-parameter family of solutions of the equation (7) system with Δ and Q as two free parameters which are, respectively, obtained from the amplitude and phase of the eigenvalue of

the scattering problem connected to the MTM; v is a dimensionless quantity ($|v| < 1$) given by

$$v = \frac{1 - \Delta^4}{1 + \Delta^4} \tag{31}$$

that determines the velocity of the soliton. The parameter Q ($0 < Q < \pi$) gives the location of the soliton in the band-gap and determines its width: $Q = \pi/2$ corresponds to a soliton with centre frequency in the middle of the gap reducing to the slow Bragg soliton of Leung (1985); the limit $Q \to 0$ corresponds to soliton-like solutions at the top of the gap reducing to the NL Schrödinger one-soliton solution of the NL PDE (Sipe & Winful, 1988), whereas the limit $Q \to \pi$ corresponds to plane-wave solutions. The generalized (*i.e.* the SP is not neglected) soliton-like solution $\bar{\mathcal{E}}(z, t)$ is built from the soliton solutions ψ of the MTM given by equation (18),

$$\bar{\mathcal{E}} = \mathcal{A}\psi \exp[i\vartheta(\xi)], \tag{32a}$$

with

$$\mathcal{A} = \frac{1}{\left(1 + R_+ + R_-\right)^{1/2}}, \tag{32b}$$

$$R_\pm = \frac{S}{4X}\,\frac{(1 \pm v)^2}{1 - v^2}, \tag{32c}$$

$$\exp[i\vartheta(\xi)] = \left[-\frac{\exp(2\bar{\kappa}\xi \sin Q) + \exp(\mp iQ)}{\exp(2\bar{\kappa}\xi \sin Q) + \exp(\pm iQ)}\right]^s, \tag{32d}$$

$$s = \frac{R_+ - R_-}{\mathcal{A}^2}. \tag{32e}$$

The solitons given by equation (32) are called self-transparency solitons. We note that the NL interaction effects appear in equation (32) mainly through the quantities $R_\pm$ *via* the ratio $S/4X$. Fig. 8 shows the time evolution of the shape of a slow Bragg soliton formed in the 1D-PC.

These soliton-like solutions can be pictured by an effective particle (Martijn de Sterke & Sipe, 1989) with a charge **q** and a momentum **p**,

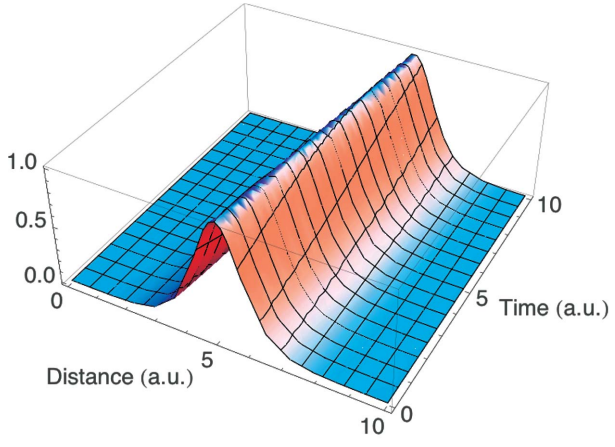

Figure 8
Time evolution of the shape of a slow Bragg soliton in arbitrary units, formed in the 1D-PC in the NL regime.

$$\mathbf{q} = \int_{-\infty}^{+\infty} \left(\mathcal{E}_+^* \mathcal{E}_+ + \mathcal{E}_-^* \mathcal{E}_-\right) \mathrm{d}z, \tag{33}$$

$$\mathbf{p} = -i \int_{-\infty}^{+\infty} \left(\mathcal{E}_+^* \partial_z \mathcal{E}_+ + \mathcal{E}_-^* \partial_z \mathcal{E}_-\right) \mathrm{d}z. \tag{34}$$

Using equation (7), it follows

$$\partial_z \mathbf{q} = 2\,\mathrm{Im}(K)\,\mathbf{q} \tag{35}$$

and

$$\partial_t \mathbf{p} = 2\,\mathrm{Im}(K)\,\mathbf{p}. \tag{36}$$

It appears that, in the absence of loss or gain, both momentum and charge will be conserved quantities, otherwise they vary exponentially with time. From these equations it can be shown that the important parameter Q satisfies

$$\partial_t Q = 2\,\mathrm{Im}(K)\,Q. \tag{37}$$

From (37) it follows that the width of the soliton, which is determined by Q, depends exponentially on time while its velocity v is still undetermined. Detailed analysis concerning the behaviour of gap solitons in the 1D-PC made up with NL media with loss and gain are given by Martijn de Sterke & Sipe (1991).

As mentioned previously, the velocity v can be regarded as a free parameter; in other words, by choosing the conditions appropriately, it should be possible to obtain very slow solitons, and even stationary solitons, up to solitons moving at about the speed of light. Low velocity ($v \approx 0$) means that energy will be transported very slowly in the manner of the self-induced transparency (SIT) observed in resonant pulse propagation in atoms (McCall & Hahn, 1967); one can then speak about Bragg SIT. Let us mention the possible existence of multi-soliton-like solutions of the time-dependent NL problem.

We now turn to the study and the conditions of a possible soliton under X-FEL pulse irradiation. First let us outline that the problem of finding the right features of the incident pulse and the appropriate conditions to give rise to a given soliton is far from trivial. For a finite-length MIM with N unit cells (bilayers), Martijn de Sterke & Sipe (1989) have given the following criteria to satisfy for the occurrence of a gap soliton,

$$N^2 \Delta n_\mathrm{L} \Delta n_\mathrm{NL} \geq 1, \tag{38}$$

where Δn_L is the magnitude of the varying term of the refractive index and Δn_NL is the maximum NL change in the refractive index. Let us also emphasize that the problem of the soliton stability is a difficult task (Hwang *et al.*, 2011), out of the domain of this paper.

4.2.2. Optical switching. The dynamics of a NL 1D-PC offers the possibility of a large variety of mechanisms that are very attractive for practical applications: optical limiting and switching, pulse generation or reshaping, *etc.* In the following we consider the optical limiting and switching (OLS) in further detail because of its potential interest in X-ray technology. OLS results from a dynamical change of the NL 1D-PC response to an incident field intensity. To understand the

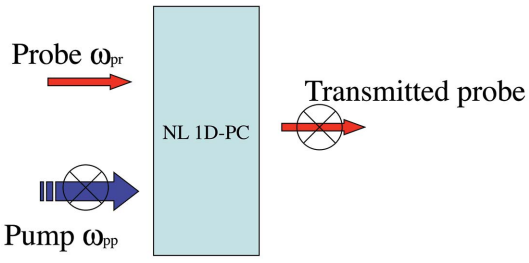

Figure 9
Scheme for an optical switching with a NL 1D-PC with negative coefficient. The NL Kerr effect is induced by the pump beam and can allow the transmission of the probe beam. In the absence of pump, there is no transmitted probe; this case is illustrated by the cross on the arrows.

principle of the OLS mechanism, it is convenient to consider the frequency domain. Here, the width of the forbidden gap (Bragg domain), GW, is proportional to the difference of the dielectric constants $\Delta\varepsilon_{ab}$ between material *a* and material *b*. Let us assume that one of the materials, say *a*, presents a NL Kerr-like behaviour with positive coefficient, *i.e.* its dielectric constant increases with the incident field intensity $\bar{E}$ while the other material shows a linear behaviour. Then, as $\bar{E}$ increases, GW increases too, so that a dynamical widening of the gap occurs. If the carrier frequency of the incident radiation is tuned at the band edge, then a larger domain of frequency of the incident pulse will fall inside the forbidden gap until forbidding the complete propagation of the pulse. This mechanism described by Scalora *et al.* (1994) forms the basis of an intensity-driven OLS.

For a NL behaviour with negative coefficient, switching can occur from the linear material in the pump/probe scheme sketched in Fig. 9: a strong pump pulse of carrier frequency ω_{pp} far below the gap and of intensity $\bar{E}_{pp}$ inducing the nonlinearity and a probe pulse of carrier frequency ω_{pr} inside the gap but near the band edge and of intensity $\bar{E}_{pr} \ll \bar{E}_{pp}$ are incident on the 1D-PC. Initially (*i.e.* without pumping) the probe pulse is not transmitted. For negative coefficient, under pump beam irradiation, the bandwidth GW decreases and over a certain value of $\bar{E}_{pp}$ the probe frequency ω_{pr} may exit the gap leading to a transmission of the probe beam. This process, which can be encountered with the negative NL coefficient of Ti in our example, may form the basis of an X-ray switch.

5. Conclusion

Ultra-short or ultra-intense X-ray pulses delivered by an X-FEL propagating within a 1D-PC opens the way to observation of many phenomena never encountered in the X-ray regime. In fact, none of the phenomena considered in this paper have been shown until now and their observation is technically challenging. Considering the LIR, measurement of the intensity of a reflected single pulse remains tricky. Nevertheless, techniques such as those implemented at the TIMEX end-station in the FERMI X-FEL facility to measure the reflectivity (Bencivenga *et al.*, 2014) can be envisaged to test our model.

When NL is incorporated into the 1D-PC at HIR, it has been shown that it becomes possible to control dynamically the propagation of an ultra-intense X-ray pulse. NL effects are generally studies both experimentally and theoretically for lossless media; in the X-ray domain and in particular for the soft X-ray range, the consequences of absorption on the NL effects are difficult to forecast in the CW theory framework without intensive numerical computation. For this purpose, calculations implementing the transfer matrix method extended to Kerr NL in a way similar to that shown by Li *et al.* (2015) could be envisaged. From an experimental point of view, to test NL effects, techniques borrowed from the optical domain involving pulse compression with cross-phase modulation should be implemented (Martijn de Sterke, 1992).

APPENDIX A

With the assumptions mentioned in the main text, the stationary version of the PDE system given by equation (7) becomes, at the *p*th Bragg resonance,

$$i\partial_z\mathcal{E}_\pm(z) = \mp\bar{\alpha}\left[\left(\left|\mathcal{E}_\pm(z)\right|^2 + 2\left|\mathcal{E}_\mp(z)\right|^2\right)\right]\mathcal{E}_\pm(z) + \bar{\kappa}\mathcal{E}_\mp(z), \tag{39}$$

with

$$\bar{\alpha} = \frac{k^2}{\kappa}\,2\pi\bar{\chi}^{(3)}, \qquad \bar{\kappa} = \frac{k^2}{\kappa}\,2\pi\Delta\chi^{(1)}u_p. \tag{40}$$

The quantity $T = |\mathcal{E}_+(z)|^2 - \left|\mathcal{E}_-(z)\right|^2$ corresponding to the transmitted flux is a conserved quantity (*i.e.* z-independent). Indeed, setting $\mathcal{E}_\pm(z) = |\mathcal{E}_\pm(z)|\exp[\pm\varphi_\pm(z)]$ and substituting into equation (39) gives, after separation of the real and imaginary parts,

$$\partial_z\left|\mathcal{E}_\pm(z)\right| = \bar{\kappa}\left|\mathcal{E}_\mp(z)\right|\sin\psi \tag{41}$$

and

$$\left|\mathcal{E}_\pm(z)\right|\partial_z\varphi_\pm = \bar{\kappa}\left|\mathcal{E}_\mp(z)\right|\cos\psi + \bar{\alpha}\left\{\left[\left|\mathcal{E}_\pm(z)\right|^2 + 2\left|\mathcal{E}_\mp(z)\right|^2\right]\right\}\left|\mathcal{E}_\pm(z)\right|, \tag{42}$$

where $\psi(z) = \varphi_+(z) - \varphi_-(z)$ at the Bragg resonance. Elimination of $\psi(z)$ from equations (41) and (42) gives the constant of propagation T. Introducing T in (39) leads to

$$\left[\partial_z\left|\mathcal{E}_+(z)\right|^2\right]^2 = 4\left|\mathcal{E}_+(z)\right|^2\left[\left|\mathcal{E}_+(z)\right|^2 - T\right] \times\left\{\bar{\kappa}^2 - 9\bar{\alpha}^2\left|\mathcal{E}_+(z)\right|^2\left[\left|\mathcal{E}_+(z)\right|^2 - T\right]\right\}. \tag{43}$$

Using the following new quantities,

$$\rho = \frac{\left|\mathcal{E}_+(z)\right|^2}{\left|\mathcal{E}_-(z)\right|^2}, \quad Z = \frac{2z}{L}, \quad N = \frac{2}{3\bar{\alpha}}, \quad I_{\rm out} = \frac{T}{N},$$

equation (39) can be rewritten

$$\frac{\mathrm{d}\rho}{\mathrm{d}Z} = \pm\left\{\rho(\rho - I_{\rm out})\left[(\bar{\kappa}L)^2 - 4\rho(\rho - I_{\rm out})\right]\right\}^{1/2}, \tag{44}$$

that is taking into account the 'standard' boundary conditions, equation (27). Equation (44) gives

$$\int_0^{\infty} \frac{\mathrm{d}\rho}{\left\{\rho(\rho - I_{\rm out})\left[(\bar{\kappa}L)^2 - 4\rho(\rho - I_{\rm out})\right]\right\}^{1/2}} = 2, \qquad (45)$$

where $\rho_0^{\pm}$ are the two roots of the binomial equation $(\bar{\kappa}L)^2 - 4\rho(\rho - I_{\rm out}) = 0$.

Evaluation of the integral on the left-hand side of equation (45) depends on the relative value of the roots of the quadric polynomial under the root square. In most usual situations these roots are real and satisfy

$$\rho(Z = 2) \rightarrow \infty > \rho_0^{+} > I_{\rm out} > 0 > \rho_0^{-}. \qquad (46)$$

In this condition, the integral on the left-hand side of equation (45) can be found by using the method given by Byrd & Friedman (1971). After some algebra,

$$\rho(Z) = \frac{I_{\rm out}}{2}\left\{1 + nd[u(Z)/m]\right\}, \qquad (47)$$

$nd[u(Z)/m]$ being the inverse of the delta amplitude of the Jacobian elliptic (cnoidal) function $dn[u(Z)/m]$ (Byrd & Friedman, 1971), where the modulus m is given by

$$m = \left[\frac{(\bar{\kappa}L)^2}{(\bar{\kappa}L)^2 + I_{\rm out}^2}\right]^{1/2} \qquad (48)$$

and

$$u(Z) = 2\left[(\bar{\kappa}L)^2 + I_{\rm out}^2\right]^{1/2}\left(1 - \frac{Z}{2}\right). \qquad (49)$$

The quantity $\rho(Z = 0)$ corresponds to normalized input intensity $I_{\rm in}$ and from equation (47) one deduces the relation between $I_{\rm out}$ and $I_{\rm in}$,

$$I_{\rm out} = \frac{2I_{\rm in}}{1 + nd\left\{2\left[(\bar{\kappa}L)^2 + I_{\rm out}^2\right]^{1/2}/m\right\}}. \qquad (50)$$

In the NL regime, one recovers the well known expression for the transmission at Bragg resonance,

$$I_{\rm out} = I_{\rm in}\,\mathrm{sech}^2(\bar{\kappa}L). \qquad (51)$$

References

Aceves, A. B. & Wabnitz, S. (1989). *Phys. Lett. A*, **141**, 37–42.
André, J.-M. & Jonnard, P. (2015). *J. Opt.* **17**, 085609.
André, J.-M., Le Guen, K. & Jonnard, P. (2014). *Laser Phys.* **24**, 085001.
Authier, A. (2003). *Dynamical Theory of X-ray Diffraction. IUCr Monographs on Crystallography* No. 11. Oxford University Press.
Bencivenga, F., Principi, E., Giangrisostomi, E., Cucini, R., Battistoni, A., D'Amico, F., Di Cicco, A., Di Fonzo, S., Filipponi, A., Gessini, A., Gunnella, R., Marsi, M., Properzi, L., Saito, M. & Masciovecchio, C. (2014). *Sci. Rep.* **4**, 4952.
Beye, M., Schreck, S., Sorgenfrei, F., Trabant, C., Pontius, N., Schüssler-Langeheine, C., Wurth, W. & Föhlisch, A. (2013). *Nature (London)*, **501**, 191–194.
Bushuev, V. A. (2008). *J. Synchrotron Rad.* **15**, 495–505.
Bushuev, V. & Samoylova, L. (2011). *Nucl. Instrum. Methods Phys. Res. A*, **635**, S19–S23.
Byrd, P. F. & Friedman, M. D. (1971). *Handbook of Elliptic Integrals for Engineers and Scientists.* Berlin/Heidelberg: Springer-Verlag.
Chen, W. & Mills, D. L. (1987). *Phys. Rev. Lett.* **58**, 160–163.
Chukhovskii, F. N. & Förster, E. (1995). *Acta Cryst.* A**51**, 668–672.
Courant, R. & Hilbert, D. (1965). *Partial Differential Equations.* New York: Interscience.
Hwang, G., Akylas, T. R. & Yang, J. (2011). *Physica D*, **240**, 1055–1068.
Jonnard, P., André, J.-M., Le Guen, K., Wu, M., Principi, E., Simoncig, A., Gessini, A., Mincigrucci, R. & Masciovecchio, C. (2016). *EUV stimulated emission from MgO pumped by FEL pulses*, https://hal.archives-ouvertes.Fr/hal-01344717.
Ksenzov, D., Grigorian, S., Hendel, S., Bienert, F., Sacher, M. D., Heinzmann, U. & Pietsch, U. (2009). *Phys. Status Solidi A*, **206**, 1875–1879.
Ksenzov, D., Grigorian, S. & Pietsch, U. (2008). *J. Synchrotron Rad.* **15**, 19–25.
Larminat, P. de (2007). *Analysis and Control of Linear Systems.* Newport Beach: ISTE.
Leung, K. M. (1985). *Phys. Rev. B*, **32**, 5093–5101.
Li, H., Haus, J. W. & Banerjee, P. P. (2015). *J. Opt. Soc. Am. B*, **32**, 1456–1462.
Martijn de Sterke, C. (1992). *Opt. Lett.* **17**, 914–916.
Martijn de Sterke, C. & Sipe, J. E. (1989). *Phys. Rev. A*, **39**, 5163–5178.
Martijn de Sterke, C. & Sipe, J. E. (1991). *Phys. Rev. A*, **43**, 2467–2473.
Martijn de Sterke, C. & Sipe, J. E. (1994). *Progress in Optics*, Vol. 33, edited by E. Wolf, pp. 203–260. Amsterdam: Elsevier.
McCall, S. L. & Hahn, E. L. (1967). *Phys. Rev. Lett.* **18**, 908–911.
Mills, D. L. & Trullinger, S. E. (1987). *Phys. Rev. B*, **36**, 947–952.
New, G. (2014). *Introduction to Nonlinear Optics.* Cambridge University Press.
Orfanidis, S. J. & Wang, R. (1975). *Phys. Lett. B*, **57**, 281–283.
Palik, E. D. (1985). *Handbook of Optical Constants of Solids.* Boston: Academic Press.
Pardo, B., Megademini, T. & André, J.-M. (1988). *Rev. Phys. Appl. (Paris)*, **23**, 1579–1597.
Scalora, M., Dowling, J. P., Bowden, C. M. & Bloemer, M. J. (1994). *Phys. Rev. Lett.* **73**, 1368–1371.
Shastri, S. D., Zambianchi, P. & Mills, D. M. (2001). *J. Synchrotron Rad.* **8**, 1131–1135.
Sipe, J. E. & Winful, H. G. (1988). *Opt. Lett.* **13**, 132–133.
Ujihara, K. (1972). *J. Appl. Phys.* **43**, 2376–2383.
Wazwaz, A.-M. (2009). *Partial Differential Equations and Solitary Waves Theory.* New York: Springer.
Winful, H. G. (1985). *Appl. Phys. Lett.* **46**, 527–529.
Winful, H. G., Marburger, J. H. & Garmire, E. (1979). *Appl. Phys. Lett.* **35**, 379–381.
Yoneda, H., Inubushi, Y., Nagamine, K., Michine, Y., Ohashi, H., Yumoto, H., Yamauchi, K., Mimura, H., Kitamura, H., Katayama, T., Ishikawa, T. & Yabashi, M. (2015). *Nature (London)*, **524**, 446–449.